

Xuzhong Su 1,2,a,
Weidong Gao 1,2,b,
Xiaoxuan Qin 1,4,5,
Xinjin Liu 1,2,3,
Chunping Xie 1,2

Numerical Simulation of Fibre Tension in an Asymmetric Ring Spinning Triangle Using FEM

DOI: 10.5604/12303666.1221740

¹ School of Textile and Clothing,
Jiangnan University,
Wuxi 214122, P. R. China
^a E-mail: mfgucv@163.com
^b E-mail: gaowd3@163.com

² Key Laboratory of Eco-Textile,
Ministry of Education,
Jiangnan University,
Wuxi 214122, P. R. China

³ Jiangsu Susi Silk Limited Company,
Suqian 223700, P. R. China

⁴ School of Media and Art Design,
Wuxi City College of Vocational Technology,
Wuxi 214122, P. R. China

⁵ Jiangsu Province Intangible Cultural Heritage
Research Base,
Jiangnan University,
Wuxi 214122, P. R. China

Abstract

In the paper, numerical simulations of fibre tension in one kind of asymmetric ring spinning triangle caused by horizontal offsets of the twisting point is studied by using the finite element method (FEM). A finite element model of the asymmetric ring spinning triangle is first established according to the mechanical properties of the fibre and a geometric model of the spinning triangle. Then the distribution of fibre tension and fibre torque in the asymmetric spinning triangle with and without considering fibre buckling are simulated by using ANSYS software. Effects of the offsets on the distribution of fibre tension and torque in the spinning triangle are studied in detail. The results show that with an increase in the spinning triangle offset, the asymmetric trend of fibre tension distribution in the spinning triangle is more obvious, and the value of fibre tension is also increased, whereas the fibre torque is decreased. Meanwhile with an increase in the yarn twist factor, the value of fibre tension and torque are both greatly increased. In addition, compared with the case where fibre buckling is considered, fibre tensions and torques are considerably increased in the case where fibre buckling is not considered.

Key words: fibre tension, fibre torque, ring spinning asymmetric triangle, FEM.

to change the spinning triangle geometry actively and improve the quality of yarn has attracted great interest recently [9].

In recent years, theoretical researches on the spinning triangle have attracted more and more attention, and fruitful results have been obtained. One theoretical model of the symmetrical spinning triangle was established based on the energy method, and the distribution of fibre tension in the spinning triangle was studied [2]. However, in practical spinning, the spinning triangles are often asymmetric. Then the model was further extended to asymmetric spinning triangles by introducing shape parameters for describing the asymmetry of the spinning triangle [4, 5, 8]. However, with the energy method, some important mechanical properties of the spinning triangle are not considered due to the problem of dissipated friction energy and the mathematical complexities. Therefore the distribution of fibre tension and torque in the symmetrical ring spinning triangle were studied by FEM [3]. Motivated by all these research works above, in this paper, the mechanical behaviour of one kind of asymmetric ring spinning triangle caused by horizontal offsets of the twisting point will be studied by using FEM.

Geometric model of the spinning triangle

Geometric models of the asymmetric spinning triangle with left and right horizontal offsets of the twisting point are

shown in **Figures 2** and **3**, respectively. Here O is the twisting point, W the width of the spinning triangle, H the height of the spinning triangle, β the apex angle, N the total number of fibres in the spinning triangle, m the number of fibres on the right (left) side of the twisting point in the spinning triangle with left (right) horizontal offsets, l_1 the length of the left (right) boundary fibre in the spinning triangle with left (right) horizontal offsets, l_2 the length of the right boundary fibre in the spinning triangle with right (left) horizontal offsets, and F is the spinning tension. In order to describe the geometric skewness of the spinning triangle, a shape parameter τ is introduced in the following simulation. In **Figures 2** and **3**, τ can be given by **Equation 1**.

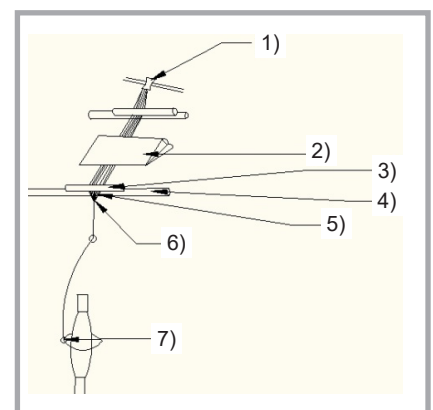


Figure 1. Ring spinning process: 1) feeding bell mouth, 2) drafting zone, 3) front top roller, 4) front roller, 5) spinning triangle, 6) twisting point, 7) traveler.

Introduction

In the process of spinning, the fibre strand first moves out from the front roller nip, in which almost all fibres are parallel to the twisting axis of the strand. Then fibres in the strand are twisted into a yarn body by the rotating of the traveller, and a spinning triangle is consequently formed (see **Figure 1**). Therefore the spinning triangle is a sensitive region in the spinning process of staple yarn. Its geometry influences the distribution of fibre tension and torque in the spinning triangle and determines the qualities of yarn [1]. The existence of the spinning triangle has a positive effect not only on the quality of yarn, but it also has a negative effect. Therefore we should control the spinning triangle reasonably. Taking appropriate measures

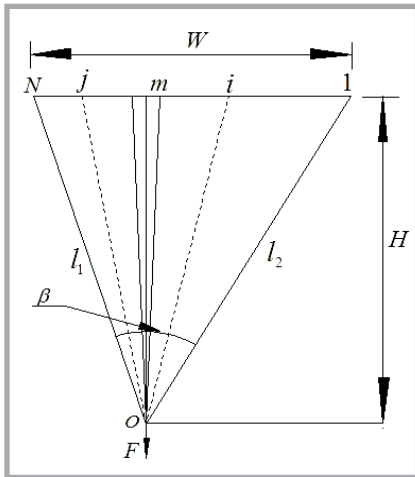


Figure 2. Geometric model of the asymmetric spinning triangle with left offset.

$$\tau = \frac{m}{N-1} \quad (1)$$

In general, the values of τ range from 0 to 1. When $\tau = 1/2$, the shape of the spinning triangle is perfectly symmetric. When $\tau = 1$, there is a right-angled shape of the spinning triangle, and when $\tau = 0$, there is a left-angled shape of the spinning triangle (see **Figure 4**). Meanwhile when $\tau > 1/2$, it describes the spinning triangle with the right offset, while when $\tau < 1/2$, it describes the spinning triangle with the left offset. For giving simulations of the spinning triangle with both the left and right offsets uniformly, the longest fibre in the spinning triangle is assumed as the number one fibre, and the shortest fibre as the number N fibre in the simulations (see **Figures 2** and **3**).

In order to investigate the mechanical performance of the asymmetric spinning triangle by using FEM, the following assumptions are made [3, 8]. The cross-section of all fibres is a circle with identical diameters. All fibres are gripped between the front roller nip and the convergence point. The fibres' stress-strain behaviour follows Hooke's law for small strain. The friction contacts between fibres and the front bottom roller and fibre slippage or migration are not considered. The initial strain of the fibre with the shortest length is set as zero. Then in order to discuss the effects of the spinning triangle offset on the distribution of fibre tension and torque in the spinning triangle, the following two different cases will be discussed.

Case 1: In this case, we suppose that the fibres are arranged at the front nip line evenly, i.e. $d = W/(N - 1)$, where d is the distance between two adjacent fi-

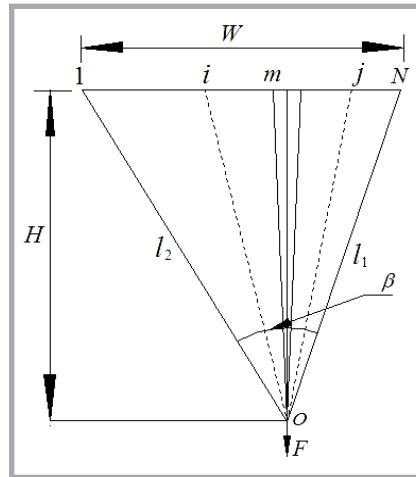


Figure 3. Geometric model of the asymmetric spinning triangle with right offset.

bres at the front nip line. Then the initial strain of the left (right) boundary fibre in the spinning triangle with left (right) horizontal offsets ε_1 is

$$\varepsilon_1 = \frac{l_1 - l_s}{l_1} \quad (1)$$

The initial strain of the right (left) boundary fibre in the spinning triangle with left (right) horizontal offsets ε_2 is

$$\varepsilon_2 = \frac{l_2 - l_s}{l_2} \quad (2)$$

Here, l_s is the length of the shortest fibre in the spinning triangle. Then for convenience of analysis, we assumed that the initial strain of the fibres in the spinning triangle ε_i can be calculated approximately as follows.

$$\varepsilon_i = \varepsilon_1 - (i-1) \frac{\varepsilon_1}{m} \quad (3)$$

for $i = 1, 2, \dots, m, m + 1$.

$$\varepsilon_j = \varepsilon_2 - (N-j) \times \frac{\varepsilon_2}{N-m-1} \quad (4)$$

for $j = m + 2, \dots, N$.

Case 2: In this case, the angle between any two adjacent fibres is supposed to be distributed evenly in the front roller nip, i.e. the angle between any two adjacent fibres α is

$$\alpha = \frac{\beta}{N-1} \quad (5)$$

Then the length of each fibre l_i in the spinning triangle can be calculated by solving the triangles. Then the initial strain of each fibre can be calculated as

$$\varepsilon_i = \frac{l_i - l_s}{l_i} \quad (6)$$

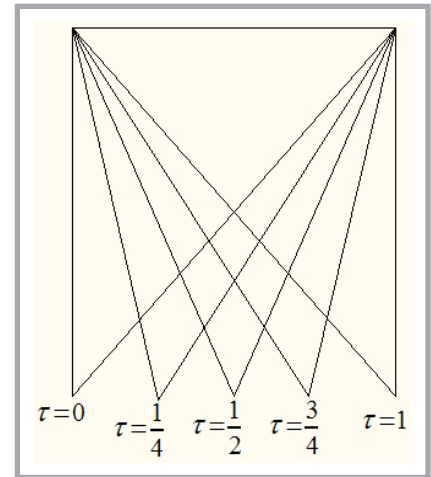


Figure 4. Geometric model of the asymmetric spinning triangle with different offsets.

Finite element model of spinning triangle

Finite element theory

In order to analyse the mechanical properties of the asymmetric spinning triangle by FEM, the element stiffness matrix of the beam elements is calculated using the direct stiffness method. The relationship of the element stiffness matrix, element node displacement and element nodal force is [6]:

$$[F^e] = [K^e] \times [\delta^e] \quad (7)$$

Here, $[F^e]$ is the element nodal force, $[K^e]$ the element stiffness matrix, and $[\delta^e]$ is the element node displacement.

The algorithm of element birth and death should be used in the simulations when the fibre bulking is considered, which can be implemented for the stiffness matrix multiplied by a small factor, which can be approximately $1.0E-6$. In order to obtain more practical results, the FULL N-R option should be open when the algorithm of element birth and death is applied. Meanwhile the death elements required should be solved first [5].

Establishment of finite element model

For obtaining a finite element model of the spinning triangle, the fibres in the spinning triangle are considered as a 3D elastic beam element. In order to make the mechanical property of the beam close to the actual fibre property, the beam element, which bears tensile, compressive, torsion and bending, is assumed to have three translation displacements and three rotation displacement structures at each one node. When fibre buckling is considered, the beam elements

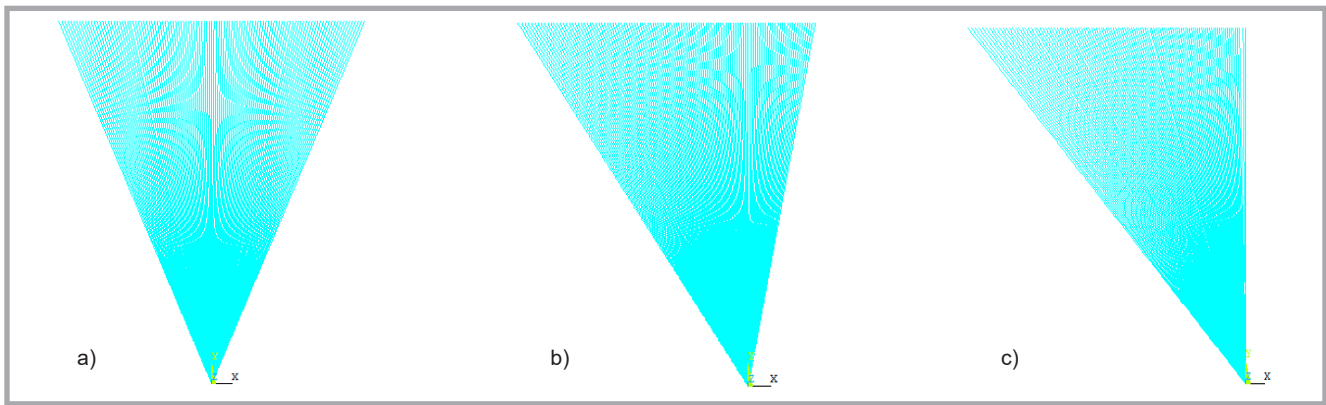


Figure 5. Finite element models of spinning triangle with different offsets. a) $\tau = 1/2$, b) $\tau = 3/4$, c) $\tau = 1$.

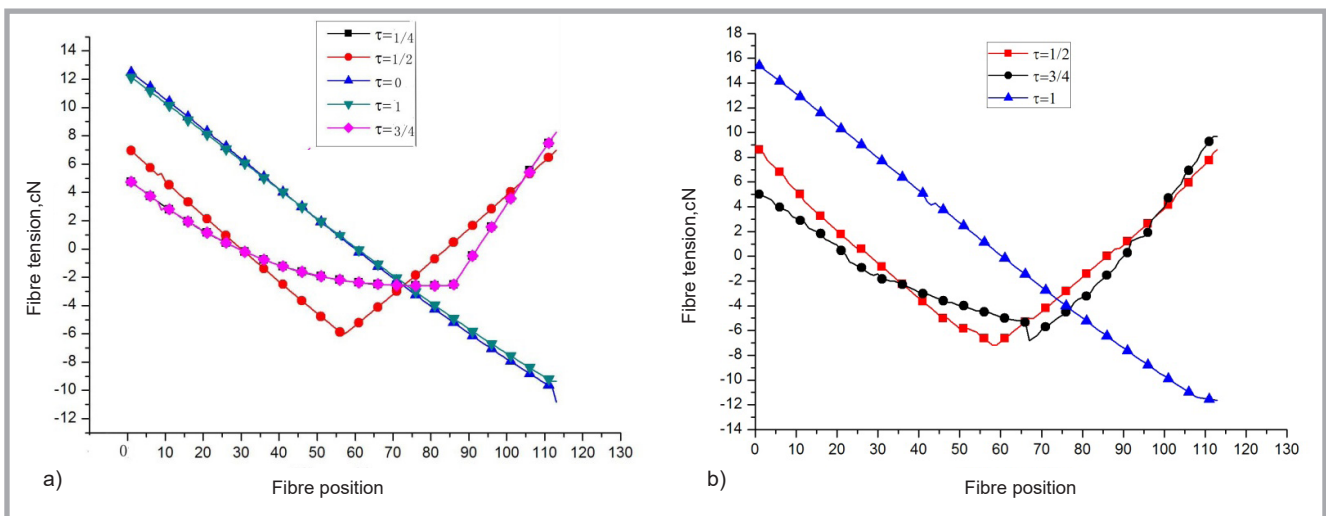


Figure 6. Fibre tension distributions under different offsets; a) twist factor 360, b) twist factor 400.

which are located in the compressed state will be set as the death element. Meanwhile the stress-strain behaviour of the beam element follows Hooke's law for small strain [6].

To illustrate the effects of the offsets of the spinning triangle on the distribution of fibre tension and torque, the spinning triangle in 14.6 tex cotton combed yarn spinning was taken as an example to study, as follows. The simulation parameters are as follows: yarn diameter: 0.143 mm, yarn twist factor: 360 and 400

Table 1. Simulation parameters.

Case	Factor twist	τ	H , mm (average value)
1	360	0	2.96
2		1/4	
3		1/2	
4		3/4	
5		1	
6	400	1/2	2.67
7		3/4	
8		1	

(the twist factor α and yarn twist T can be converted to each other as $T = \alpha / \sqrt{N}$, where N is the count of the yarn in tex), the number of fibres in the spinning triangle: $N = 113$, fibre diameter: 0.016 mm, fibre elastic modulus: 5 N/tex, fibre shear modulus: 1.35 N/tex, fibre density: 1.54 g/mm, spinning angle [3] $\beta = 2\theta$, where θ is the yarn surface-helix angle and $\tan \theta = 2\pi RT$, R the yarn radius and T the yarn twist, spinning tension: 30 cN, and the width of the spinning triangle: $W = 2.5$ mm. In the following analysis, the width of the spinning triangle is assumed to be unchanged since the ends of fibres in the spinning triangle are pressed by the nip line. Then finite element models of the spinning triangle can be obtained with different offsets, as shown in Figure 5. The other input simulation parameters are shown in Table 1. Then the distributions of fibre tension and fibre torque in the spinning triangle both with and without fibre bucking under different spinning triangle offsets will be simulated using ANSYS software.

Fibre tension distributions

Fibre tension distributions without fibre bulking

Simulation results in Case 1

Under the assumptions in case 1, simulation results of the fibre tension distribution in the spinning triangle with different offsets at two different twist factors: 360 and 400 are shown in Figure 6. It is shown that the distribution of fibre tension in the spinning triangle is symmetrical about the middle fibre when $\tau = 1/2$, while the fibre tension distribution in the spinning triangle is asymmetrical when $\tau \neq 1/2$. With an increase in τ when $\tau > 1/2$, or a decrease in τ when $\tau < 1/2$, the asymmetry of the curve is increased. Meanwhile as shown in Figure 6.a, the distribution curve of fibre tension in the spinning triangle is a coincidence for $\tau = 1$ and $\tau = 0$, or $\tau = 1/4$ and $\tau = 3/4$ due to the labelling method in the paper (see Figures 2 and 3). Therefore the fibre tension distribution in the spinning triangle at twist factor 400 is given in Figure 6.b only for $\tau = 1/2$, $\tau = 3/4$ and $\tau = 1$.

From the **Figure 6**, it is easy to see that fibre tensions at different offsets have different magnitudes, and the detail range of fibre tension is shown in **Table 2**. It is seen that the curve of fibre tensions with the right-angled or left-angled shape exhibits the largest variation. Meanwhile with an increase in the twist factor, the magnitude is also increased.

Simulation results in case 2

Under the assumptions in case 2, simulation results of the fibre tension distribution in the spinning triangle with three different offsets at two different twist factors 360 and 400 are shown in **Figure 7**. In the Figures, compared with the curve obtained in case 1, the gradient of fibre tension curve is smoother, and the value of fibre tension is a little larger. In addition, with an increase in the twist factor,

Table 2. Fibre tension variation rang under different offsets.

Twist factor	360			Twist factor 400			
	τ	1/2	3/4	1	1/2	3/4	1
Max tensile load, cN		6.90	8.20	12.10	8.60	10.50	15.40
Max compression load, cN		5.40	2.60	9.30	7.40	5.10	11.60

the magnitude of fibre tension is also increased.

According to the simulation results above, the distribution of fibre tension in the spinning triangle is symmetrical about the middle fibre in the spinning triangle without offset. That is, in the process of spinning, the fibres on left and right sides of the spinning triangle will flip to the centre of the triangle and gather in the yarn body. In this case, on the one hand, the fibres, especially the boundary fibres, in the spinning triangle

centre cannot be wrapped into the yarn body completely and form hairiness. On the other hand, there exists an angle between the fibres and yarn axis, which leads to a decrease in yarn strength.

With an increasing in left (right) offset, the fibres on the right (left) side of the spinning triangle have larger tension than that of the fibres on the left (right) side. In general, for Z (S)-twist yarn, when the “Z” (“S”) twisting affects fibres in the spinning triangle, the fibres on

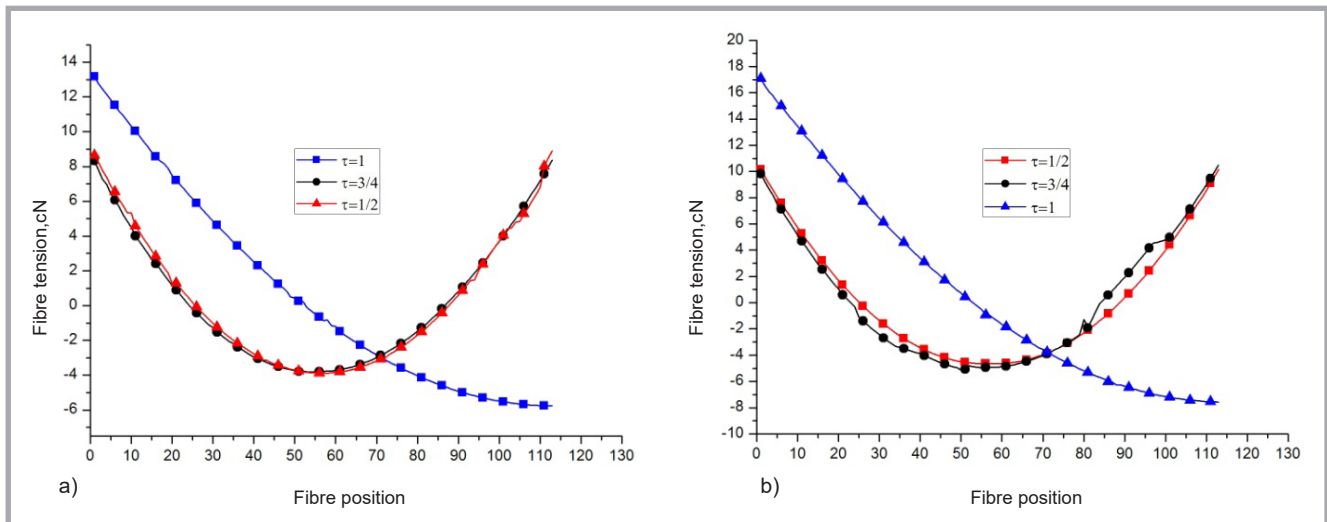


Figure 7. Fibre tension distribution under different offsets; a) twist factor 360, b) twist factor 400.

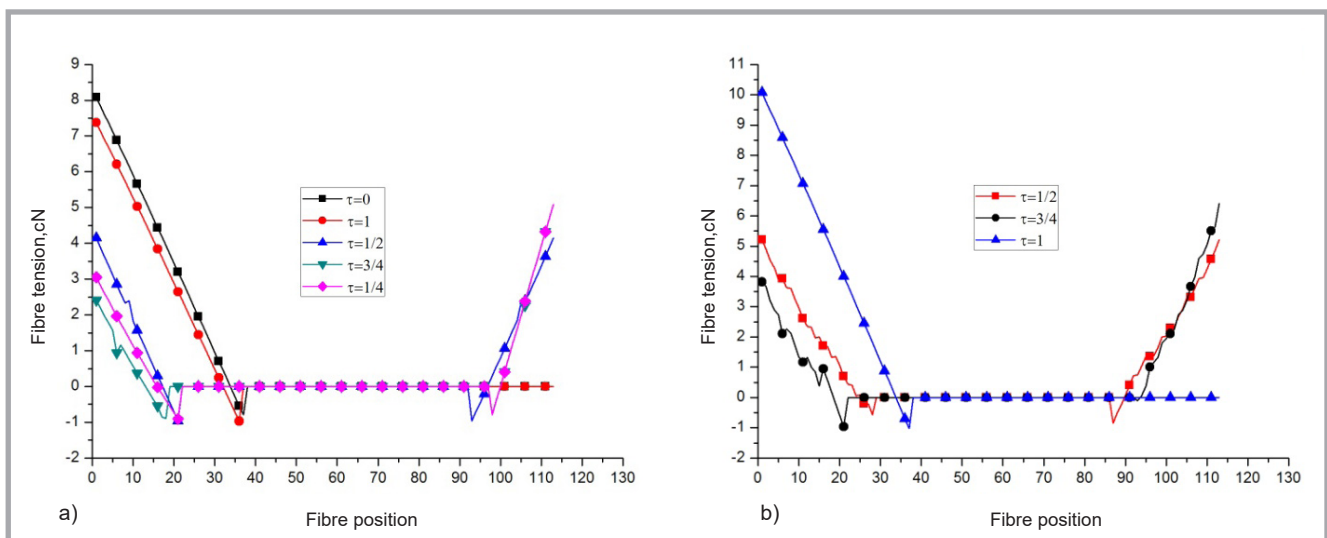


Figure 8. Fibre tension distribution under different offsets in case 1; a) twist factor 360, b) twist factor 400.

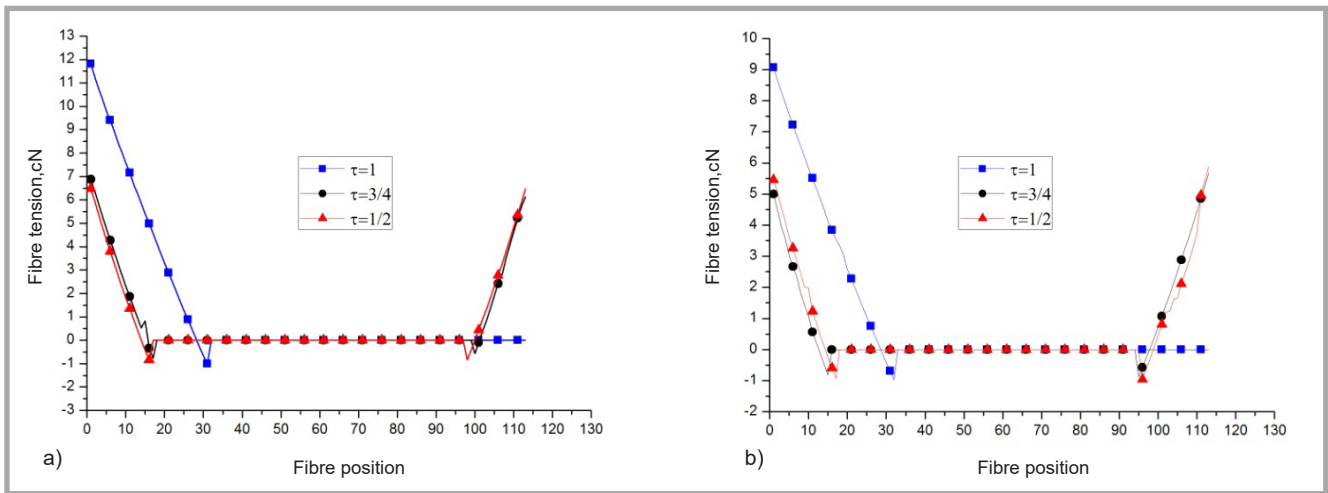


Figure 9. Fibre tension distributions under different offsets in case 2; a) twist factor 360, b) twist factor 400.

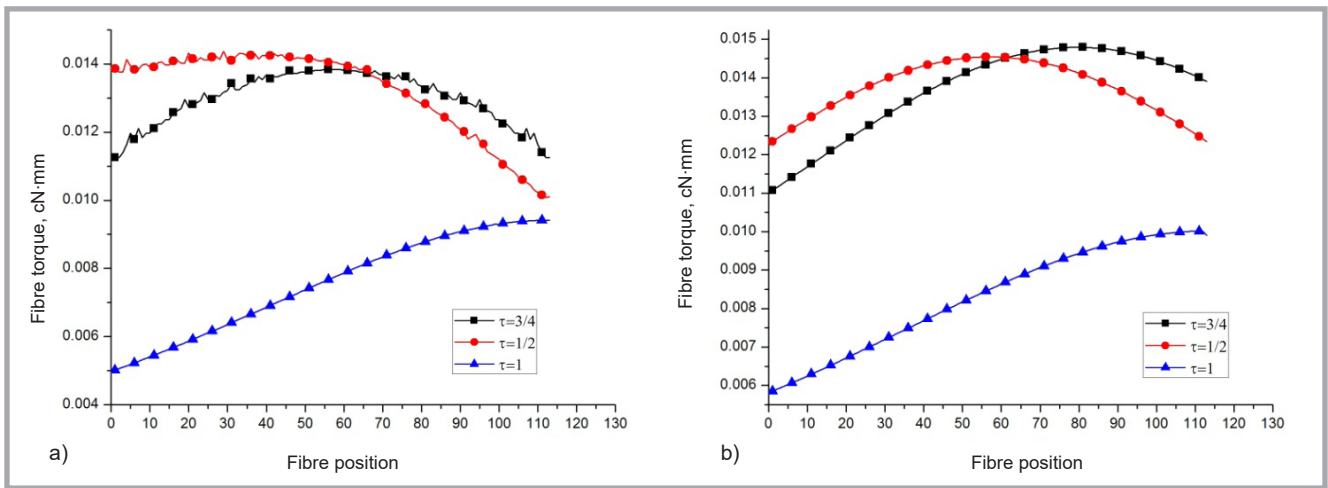


Figure 10. Fibre torque distribution under different offsets in case 1; a) twist factor 360, b) twist factor 400.

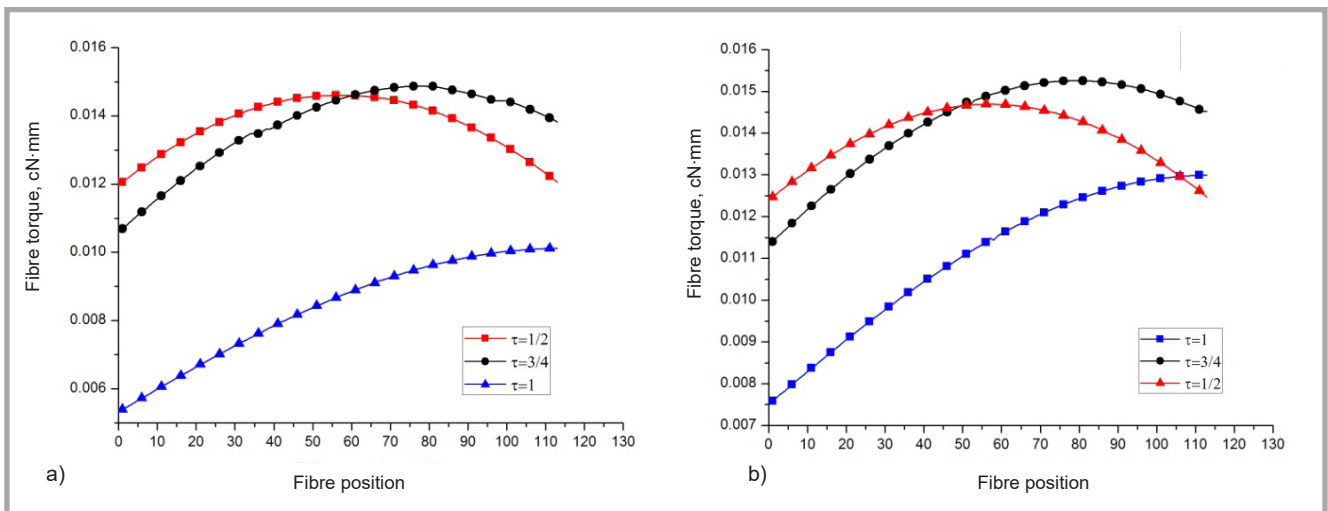


Figure 11. Fibre torque distribution under different offsets in case 2; (a) twist factor 400, (b) twist factor 400.

the right (left) side can be controlled by the pre-twisting process, i.e. there is pre-tension for fibres on the right (left) side, whereas the fibres on the left (right) side are relatively loose. Therefore the control

of fibres on the left (right) side should be strengthened through an asymmetrical spinning triangle, which can be realized by changing the horizontal offset. From the simulation results shown in **Fig-**

ures 6 and 7, fibres on the left (right) side of the spinning triangle with the right (left) offset have larger tension and can be well controlled and then wrapped into the yarn body, thereby possibly im-

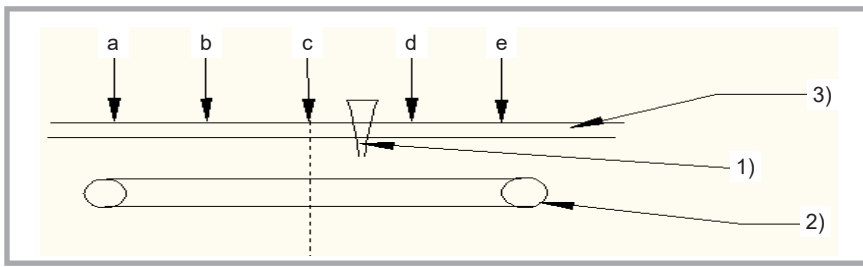


Figure 12. Practical spinning progress; 1) feeding bell mouth, 2) back top roller, 3) shifting device.

proving yarn qualities. However, with an increasing in the offset, the tension of outer fibres increases fast, and when the fibre tension increases to a certain degree and exceeds the maximum tolerance of the fibre, the fibre will be broken and not benefit yarn quality. In a word, the choice of spinning triangle offset $\tau = 3/4$ or $\tau = 1/4$ may improve JC40S yarn qualities, which will be verified in the experimental part.

Fibre tension distributions with fibre bulking

By using FEM, when fibre bulking is considered, simulation results of the fibre tension distribution in the spinning triangle with three different offsets at two different twist factors: 360 and 400 are given in **Figures 8** (see page -2) and **9** under the assumptions in case 1 and 2, respectively. From the figures, with an increase in the offset of the spinning triangle, the value of fibre tension is increased. Moreover the value of fibre tension obtained in case 2 is larger than that of in case 1. Compared to the case where fibre bucking is not considered, fibre ten-

Table 3. Measured properties of yarn with twist factor 360.

τ	Hairiness, H value	Yarn tenacity, cN/tex	Elongation at break, %
1/2	4.91	15.16	5.59
3/4	4.83	15.32	5.65
1/4	4.86	15.17	5.60
1	4.88	15.04	5.50
0	4.87	15.02	5.48

Table 4. Measured properties of yarn with twist factor 400.

τ	Hairiness, H value	Yarn tenacity, cN/tex	Elongation at break, %
1/2	4.88	15.20	5.64
3/4	4.76	15.40	5.72
1/4	4.90	15.18	5.61
1	4.85	15.16	5.59
0	4.82	15.14	5.51

sion is greatly reduced in the case where fibre bucking is considered.

Fibre torque distribution

In this section, the effects of the spinning triangle offset on the fibre torque distribution will be discussed. By using FEM, where fibre bulking is not considered, simulation results of the fibre torque distribution in the spinning triangle with three different offsets at two different twist factors: 360 and 400 are shown in **Figures 10** and **11** under the assumptions in case 1 and 2, respectively. From the figures, with an increase in the twist factor, the value of fibre torque is increased. From **Figures 10.a** and **11.a**, for the same twist factor, where the offset changes from $\tau = 1/2$ to $\tau = 3/4$, the torque of fibres which are located from 0th to 60th is gradually reduced, whereas that of fibres which are located from 61th to 113th is gradually increased. When the offset $\tau = 1$, the fibre torque is significantly reduced. That is, a suitable spinning triangle offset may reduce the yarn residual torque. However, from the simulation results of fibre tension above, the spun yarn may have poor strength and more hairiness when $\tau = 1$. Therefore in the actual spinning, the optimal spinning triangle offset should be comprehensively considered.

Experiments

14.6 tex cotton combed yarn with Z twist was spun on a FA507B ring spinning machine, and the offsets of the spinning triangle controlled by changing the position of the feeding bell mouth, see **Figure 12**. As shown in **Figure 12**, the bell mouth can be moved in the shifting device, and the offset of the spinning triangle can be changed correspondingly. In the shifting device, five key points: a, b, c, d and e are defined, and the offsets of the spinning triangle are 1, 3/4, 1/2, 1/4 and 0, correspondingly. Combed roving of 400 tex

is used as raw material, and the yarn twist factor is 360 and 400. The test instruments are listed as follows - Yarn hairiness tester: YG173A, testing speed 30 m/min, and testing length 100 m. Yarn strength tester: YG020B, stretching velocity 5 m/min, and pre-tension 7.3 cN. The test results are shown in **Tables 3** and **4**.

From **Tables 3** and **4**, we can see the comprehensive quality of 14.6 tex cotton combed yarn with Z twist is the best at both of the different twist factors when $\tau = 3/4$. From the analysis above, for Z-twist yarn, fibres on the left side can be controlled better with the right offset, while those on the right side are still controlled by the pre-twisting. Therefore with an appropriate right offset, yarn qualities can be improved with Z twist. Simultaneously with an appropriate left offset, yarn qualities would be improved with S twist. Therefore the result is consistent with the simulation results above. Meanwhile we can guess that the comprehensive quality of 14.6 tex cotton yarn with S twist would be improved when $\tau = 1/4$.

Conclusion

In this paper, the relationship between the offsets of the twisting point of the spinning triangle and the distribution of fibre tension and fibre torque in an asymmetric ring spinning triangle has been analysed by using FEM. In order to describe the asymmetric nature of the spinning triangle, the one shape parameter τ is adopted in the analysis. Values of the shape parameter τ range from 0 to 1. When $\tau > 1/2$, it denotes that the spinning triangle has a right offset, while the spinning triangle has the left offset when $\tau < 1/2$.

By using FEM, the distributions of fibre tension and fibre torque in a asymmetric ring spinning triangle with different offsets have been obtained. The simulation results show that with an increasing in the spinning triangle offset, the asymmetry of the curve is increased, as well as the magnitudes of fibre tension. Meanwhile compared with the case where fibre bucking is considered, the fibre tension is greatly increased when fibre bucking is not considered. Meanwhile with an increasing in the spinning triangle offset, fibre torque is decreased, which is beneficial for reducing yarn torque. However, with an increasing in the spinning triangle offset, the other yarn qualities may become poor. Therefore in the ac-

tual spinning, the optimal spinning triangle offset should be comprehensively considered.



Acknowledgements

This work was supported by a Project Funded by the Priority Academic Program Development of Jiangsu Higher Education Institutions (PAPD), the project of Xinjiang Uygur Autonomous Region key research and development (2016B02025-1), Henan collaborative innovation of textile and clothing industry (hnfz14002), the Natural Science Foundation of Jiangsu Province under Grant (BK20151359), Prospective industry-university-research project of Jiangsu Province (BY2016022-27, BY2015019-10), Prospective industry-university-research project of Guangdong Province (2013B090600038), Class general financial grant from the china post-doctoral science foundation (2015M581722), Postdoctoral research funding program of Jiangsu Province (1501146B).

References

1. Liu XJ, Su XZ. Research on fiber tension in ring spinning triangle [J]. *Journal of Textile Research* 2013; 34(12): 32-36.
2. Najjar SS. An Analysis of Twist Triangle in Ring Spinning [D]. University of New Wales, 1996.
3. Li SY, Xu BG, Tao XM and Feng J. Numerical analysis of the mechanical behavior of a ring-spinning triangle using the Finite Element Method [J]. *Textile Research Journal* 2011; 81(9): 959-971.
4. Hua T, Tao XM, Cheng KPS, Xu BG. Effects of Geometry of Ring Spinning Triangle on Yarn Torque Part I: Analysis of Fiber Tension Distribution [J]. *Textile Research Journal* 2007, 77(11): 853-863.
5. Hua T, Tao XM, Cheng KPS and Xu BG. Effects of Geometry of Ring Spinning Triangle on Yarn Torque: Part II: Distribution of Fiber Tension within a Yarn and Its Effects on Yarn Residual Torque [J]. *Textile Research Journal* 2010; 80(2): 116-123.
6. Hu RX, Xu DS, Li YD. ANSYS13.0 mechanical and structural finite element analysis from beginning to the proficiency [M]. Bei Jing: China Machine Press, 2011.
7. Wang XM, Li YQ and Xu HW. Structural Analysis Unit and Application [M]. Bei Jing: China Communications Press, 2011.
8. Feng J, Xu BG, Tao XM and Hua T. Theoretical Study of Spinning Triangle with Its Application in a Modified Ring Spinning System. *Textile Research Journal* 2010; 80(14): 1456-1464.
9. Liu XJ, Su XZ and Wu TT. Effects of the horizontal offset of ring spinning triangle on yarn. *Fibres and Textiles in Eastern Europe* 2013; 21, 1(97): 35-40.

Received 27.07.2015 Reviewed 31.01.2016

FILTECH 2016, Cologne

THE FILTRATION EVENT 2016

Conference, exhibition and short courses

October 11 - 13, 2016, Cologne, Germany

FILTECH 2016 Conference will feature once again the latest advances and techniques in liquid/solid and gas/particle separation (dust, gas & air filtration) in 3 days of in depth exposure. Technology and know-how transfer is a main target.

The topics are fundamentals, equipment and strategies to "Solid-Liquid Separation" by filtration and sedimentation, as well as "Air and Gas Cleaning" by filtration, setting, electrostatic precipitation, scrubbing, and "Membrane Separation Technology".

Plenary Lecture

- Prof. **Gerhard Kasper**, Karlsruhe Institute of Technology, Germany
Gas Cleaning with Pulse-Jet Filters: Emission Sources and Dust Abatement Strategies

Keynote Lectures

- Dr. **Christof Asbach**, IUTA, Germany
Long-term Stability and Energy Efficiency of Filtration Solutions
- Prof. **Anti Häkkinen**, Lappeenranta University, Finland
Role of Solid/Liquid Separation Technology in Circular Economy
- Prof. **Eiji Iritani**, Nagoya University, Japan
Approach to Membrane Filtration from the Perspective of Cake and Blocking Filtration Laws
- Prof. **Hans Theliander**, Chalmers University, Sweden
On local Cake Properties in Liquid Filtration
- Prof. **Peter Walzel**, Dr.-Ing. **Damian Pieloth**, Technical University Dortmund, Germany
Dust Removal in Scrubbers - State of the Art and Challenges
- Dr. **Wolfgang Witt**, Sympatec GmbH, Germany
Particle Size and Shape Analysis for Laboratory and Process Environment

Engineers, managers, researchers and scientists are invited to submit an Abstract for the FILTECH 2016 Conference.

FILTECH exhibition has an established track record in bringing together the technical and commercial sectors to develop global business relationships. This Exhibition is a must for all those concerned with designing, improving, selling or researching filtration and separation equipment and services. FILTECH is the international platform and solution provider for all industries covering every market segment.

One day prior to FILTECH 2016 two 1-day short courses will be held:

- **Solid/Liquid Separation** - Dr.-Ing. **Harald Anlauf** - Academic Director at the Karlsruhe Institute of Technology (KIT).
- **Fine Dust Separation** - Prof. Dr.-Ing. habil. **Eberhard Schmidt** - Full Professor for Safety Engineering/Environmental Protection at Wuppertal University.

For further details see:

www.filtech.de → Conference